

Serotonergic Input into the Cerebellar Cortex Modulates Anxiety-Like Behavior

Pei Wern Chin¹ and  George J. Augustine^{1,2}

¹Lee Kong Chian School of Medicine, Nanyang Technological University, Singapore 308232, Singapore and ²Temasek Life Sciences Laboratory, Singapore 117604, Singapore

Because of the important roles of both serotonin (5-HT) and the cerebellum in regulating anxiety, we asked whether 5-HT signaling within the cerebellum is involved in anxiety behavior. Physiological 5-HT levels were measured *in vivo* by expressing a fluorescent sensor for 5-HT in lobule VII of the cerebellum, while using fiber photometry to measure sensor fluorescence during anxiety behavior on the elevated zero maze. Serotonin increased in lobule VII when male mice were less anxious and decreased when mice were more anxious. To establish a causal role for this serotonergic input in anxiety behavior, we photostimulated or photoinhibited serotonergic terminals in lobule VII while mice were in an elevated zero maze. Photostimulating these terminals reduced anxiety behavior in mice, while photoinhibiting them enhanced anxiety behavior. Our findings add to evidence that cerebellar lobule VII is a topographical locus for anxiety behavior and establish that 5-HT input into this lobule is necessary and sufficient to bidirectionally influence anxiety behavior. These results represent progress toward understanding how the cerebellum regulates anxiety behavior and provide new evidence for a functional connection between the cerebellum and the serotonin system within the anxiety circuit.

Key words: anxiety; cerebellum; serotonin

Significance Statement

This is the first analysis of the involvement of the neuromodulator, serotonin, in the cerebellum during anxiety behavior. Our results reveal that serotonin regulates anxiety behavior. This offers new insight into the role of serotonin in the cerebellum, as well as illuminating how the cerebellum interacts with the rest of the brain to regulate anxiety. Our results are important for future use of serotonin-related pharmacological therapeutics, such as selective serotonin-reuptake inhibitors, in treating anxiety in humans.

Introduction

The cerebellum is traditionally known for its role in coordinating motor behavior and balance (Thach et al., 1992; Morton and Bastian, 2004). These conclusions arose from extensive evidence demonstrating that cerebellar lesions or dysfunctions result in distinct motor-related pathologies, such as motor imbalance, ataxia, and dystonia (Thach et al., 1992; Ito, 2002; Koeppen, 2018; Wang et al., 2023). Such studies led to the widespread

impression that the cerebellum is solely involved in orchestrating motor-related tasks in the brain. However, a substantial body of more recent evidence also indicates that the cerebellum is involved in a variety of non-motor functions, including anxiety (Zhu et al., 2011; Badura et al., 2018; Carta et al., 2019; Frontera et al., 2020; Jackman et al., 2020; Baek et al., 2022; Cutando et al., 2022).

Many clinical studies have implicated the cerebellum in anxiety disorders (Cassimjee et al., 2010; Roy et al., 2013; Moreno-Rius, 2018). Lesions or pathologies of the human cerebellar vermis are associated with anxiety-related impairments (Richter et al., 2005). Similarly, lesions of the cerebellar vermis disrupt anxiety behavior in rats (Supple et al., 1987; Bobée et al., 2000). A causal role for the cerebellum in regulating anxiety behavior has been established through a variety of experimental manipulations of the cerebellum in rodents (Ha et al., 2016; Helgers et al., 2020; Rudolph et al., 2020).

The serotonin (5-hydroxytryptamine, or 5-HT) neuromodulatory system is also known to be involved in anxiety (Cassano et al., 2002; Moulédous et al., 2018; Olivier and Olivier, 2020; Zangrossi et al., 2020). Extensive evidence demonstrates that

Received Sept. 24, 2024; revised Nov. 15, 2024; accepted Dec. 5, 2024.

Author contributions: P.W.C. and G.J.A. designed research; P.W.C. performed research; P.W.C. analyzed data. P.W.C. and G.J.A. wrote the paper.

We thank Karen Chung for her invaluable technical support, Drs. Jinsook Kim and Arong Jung for their help with cerebellar slice imaging, and Drs. Jinxia Wan and Yulong Li (Peking University) for kindly providing us with their GRAB_{5HT2h} sensor prior to its publication. The experimental work described in this paper represents part of Ph.D. thesis of P.W.C. at Nanyang Technological University. This work was supported by research grant MOE2017-T3-1-002 from the Singapore Ministry of Education and by the Temasek Life Sciences Laboratory.

The authors declare no competing financial interests.

P.W.C.'s present address: School of Arts and Sciences, University of Pennsylvania, Philadelphia, Pennsylvania 19104.

Correspondence should be addressed to George J. Augustine at george_augustine@tll.org.sg.

<https://doi.org/10.1523/JNEUROSCI.1825-24.2024>

Copyright © 2025 the authors

serotonergic neurons in the dorsal and median raphe nuclei regulate anxiety behavior: for example, activating these neurons induces anxiogenic effects in rodents (Teissier et al., 2015; Marcinkiewicz et al., 2016; Abela et al., 2020). In the cerebellum, 5-HT fibers are the third largest population of afferent fibers (Saitow et al., 2013; Oostland and Hooft, 2016). These 5-HT afferents are distributed throughout the cerebellum and primarily originate from the raphe nuclei, including the rostral raphe (dorsal and median raphe) and the caudal/medullary raphe nuclei (Shinnar et al., 1975; Pierce et al., 1977). 5-HT has been found to act on cerebellar neurons (Mitoma et al., 1994; Dieudonné and Dumoulin, 2000; Dean et al., 2003; Fleming and Hull, 2019) and also mediates stress-induced dystonia in the deep cerebellar nuclei (Kim et al., 2021). It is possible that 5-HT modulation of aversive behavior, such as anxiety, could also exist within the cerebellar cortex.

Despite substantial evidence indicating roles for both the cerebellum and 5-HT in anxiety, the potential role of neuromodulation of the cerebellum by 5-HT during anxiety behavior has not been examined. Here we have considered this possibility by measuring and manipulating 5-HT levels in lobule VII of the mouse cerebellum while examining anxiety behavior. We first employed a 5-HT-specific fluorescence sensor (Deng et al., 2024) to measure endogenous 5-HT levels in the cerebellum and found an inverse relationship between 5-HT and anxiety levels. Next, we used optogenetics to control serotonergic input to the cerebellum and found that local photostimulation of serotonergic neurons reduced anxiety behavior, while photoinhibition of these neurons enhanced anxiety behavior. Our results indicate that 5-HT input to the cerebellum is both sufficient and necessary to regulate anxiety behavior.

Materials and Methods

Animals and housing. All mouse procedures were conducted according to the NTU Institutional Animal Care and Use Committee (IACUC) guidelines. Mice were housed in a 12 h light/dark cycle (0700–1900 light on, 1900–0700 light off) with food and water provided *ad libitum*. Male mice were used for all experiments (Chin and Augustine, 2023). All mice were group housed, unless otherwise specified, and were 2–3 months old at the time of stereotaxic surgery. C56/BL6J wild-type mice were used for GRAB_{5HT2h} fiber photometry measurements. To photostimulate or photoinhibit serotonergic input to the cerebellum, heterozygous ePet-Cre transgenic mice (JAX #012712; Scott et al., 2005) were crossed with mice where a *loxP*-flanked STOP cassette controlled expression of channelrhodopsin2 (ChR2) fused to YFP (homozygous, line Ai32; JAX #012569; Madisen et al., 2012) or archaerhodopsin (Arch) fused to YFP (heterozygous, line Ai35; JAX #012735; Madisen et al., 2012) to specifically express ChR2 or Arch in serotonergic neurons. Littermates not expressing either Cre recombinase (only *loxP*-flanked ChR2 or Arch) or Arch (only Cre recombinase) were used as controls for optogenetic experiments, as indicated.

Expression of GRAB sensor in the cerebellum. The fluorescent sensor, GRAB_{5HT2h}, was employed to monitor 5-HT levels (Deng et al., 2024). To express GRAB_{5HT2h} in lobule VII neurons, 200–300 nl of AAV9-hSyn1-5HT3.5(h-S06) (WZ Biosciences) was injected into lobule VII at AP -7.60 or -8.15 mm, ML 0.00 mm, DV -0.40 mm for 2- or 3-month-old mice. For intracranial drug microinjection experiments, 500 nl of AAV9-hSyn1-5HT3.5(h-S06) was injected into lobule VI at AP -7.35 mm, ML 0.00 mm, DV -0.60 mm. Virus was injected at a flow rate of 1 nl/s, using glass pipettes attached to a 5 μ l Hamilton syringe (Hamilton Company) and a stereotaxic pressure injector (World Precision Instruments). Mice were administered the antibiotic drug, Baytril, and anti-inflammatory drug meloxicam via drinking water and monitored for proper recovery for 1 week postsurgery.

GRAB sensor measurements in cerebellar slices. Acute cerebellar slices were prepared 2–3 weeks after viral transduction to allow adequate time for expression of GRAB_{5HT2h}. Mice were deeply anesthetized with isoflurane and killed via decapitation, and their brains were harvested for slice preparation. Sagittal cerebellar brain slices (300 μ m thickness) were prepared with a vibratome (VT 1000S; Leica) in oxygenated cutting solution (in mM: 250 sucrose, 10 glucose, 26 NaHCO₃, 4 MgCl₂, 3 myo-inositol, 2.5 KCl, 2 sodium pyruvate, 1.25 NaHPO₄, 0.5 ascorbic acid, 1 kynurenic acid, 0.1 CaCl₂). Slices were incubated at 34°C in oxygenated (95% O₂/5% CO₂) artificial cerebrospinal fluid (aCSF; in mM: 126 NaCl, 24 NaHCO₃, 1 NaH₂PO₄, 10 glucose, 2.5 KCl, 2 MgCl₂, 0.4 ascorbic acid, 2.5 CaCl₂) for 30–60 min prior to fluorescence imaging.

To image GRAB_{5HT2h} fluorescence, slices were placed in a recording chamber and continuously perfused with oxygenated aCSF at room temperature (22–24°C). Images were obtained using a two-photon microscope (Olympus FV-1000; 950 nm excitation wavelength). A *z*-stack image set was first obtained while slices were in 5-HT-free aCSF; aCSF containing 5-HT (50 nM–50 μ M) was then perfused into the recording chamber for 5 min prior to acquisition of another set of images. Between applications of 5-HT, slices were treated with 5-HT-free aCSF for 5 min to remove any residual 5-HT.

All fluorescent images were processed and quantified using Fiji macros (Schindelin et al., 2012). Regions of interest (ROIs; 60 μ m \times 60 μ m) within the molecular layer and granule cell layer were identified for quantification, whereas individual Purkinje cell somata were pseudorandomly selected for quantification. Changes in fluorescence produced by 5-HT treatment, in comparison with basal conditions, were normalized by dividing sensor fluorescence measured at basal conditions (5-HT-free aCSF), $\Delta F/F_0$, where F_0 is the basal fluorescence in the absence of 5-HT. Background fluorescence, measured in areas of the cerebellar slice not expressing any GRAB sensor, was subtracted prior to calculating $\Delta F/F_0$. Half-maximal effective concentrations (EC₅₀) for 5-HT activation of the GRAB_{5HT} sensor were determined by fitting sigmoidal dose–response curves to the $\Delta F/F_0$ values calculated for all three cerebellar layers.

In vivo measurement of GRAB sensor fluorescence. In vivo measurements of GRAB_{5HT2h} fluorescence were made via fiber photometry. For delivery of light during these measurements, as well as during optogenetic experiments (see below), light was delivered via an optical fiber cannula that was implanted at lobule VII (anterior–posterior $-7.80/-8.25$ mm, medial–lateral 0.00 mm, dorsal–ventral -0.10 mm for 2- or 3-month-old mice). The cannula was fixed to a screw anchor on the skull with C&B Metabond (Parkell) and black dental cement (Lang Dental). To inject 5-HT or 5-HT receptor antagonist solutions into the cerebellum, a needle cannula (27 gauge, regular bevel 11°) was implanted into lobule VI (AP -6.85 to -6.95 mm, ML 0.00 mm, DV -1.50 mm) at an angle of 25°, with the beveled side of the needle facing the injection site. A homemade dust cap with 200- μ m-diameter stainless steel wire was passed through the opening of the needle cannula to prevent blockage caused by dust or mouse tissue. An optical fiber cannula was then implanted at lobule VI (AP -7.45 mm, ML 0.00 mm, -0.30 mm).

Fiber photometry hardware was constructed with 405 and 470 nm LEDs, LED drivers (LEDD1B), fluorescence filter cubes housing excitation filters (FBH405-10 and MF469-35), dichroic and long-pass dichroic mirrors (MD498 and DMLP425R), emission filter (MF525-39, Thorlabs), 0.5 NA optical fiber patch cables, collimators (F950FC-A), a photodetector (Photon Counting PMT Detection System; Horiba Scientific), and a National Instruments Data Acquisition (NI-DAQ) device (USB-6002, National Instruments). Bonsai, an open-source software interface (<https://open-ephys.org/bonsai>), was used to control light delivery, as well as to synchronize, time stamp, and acquire fluorescence signals (200 Hz sampling frequency) along with behavioral video recording (30 frames per second). Rectangular pulses of 405 and 470 nm light (5 Hz) were alternately delivered in an interleaved pattern to excite the GRAB_{5HT2h}. LED power outputs were empirically determined for each animal prior to each session and were limited to between 30 and 90 μ W (470 nm) and 20–65 μ W (405 nm). A 2 m optical fiber patch cable (200 μ m core diameter, 0.5 NA; Thorlabs) was used to connect the optical fiber cannula on the animal to the fiber photometry system via a black

ceramic sleeve (Doric Lenses). The optical fiber was photobleached before each day of recording to minimize autofluorescence.

Videos were tracked on Bonsai and data were further processed in MATLAB for time-locked behavioral analysis of photometry data. Custom MATLAB scripts were used for analyses, with code adapted from that developed by the labs of Talia Lerner (<https://github.com/talialerner/Photometry-Analysis-Shared>) and Thomas Kash (<https://groups.google.com/g/bonsai-users/c/utRQdqvKK-g/m/R6BxgC2hFQA>). Both were obtained from the Bonsai Google Forum. Fluorescence emission signals collected at 200 Hz were deinterleaved into 405 nm excited and 470 nm excited signals. The 405 nm signal was used as an isosbestic signal to account for potential artifacts caused by animal movement. To correct for photobleaching over time, the 405 nm signal was scaled to the 470 nm signal, using exponential regression, to generate a fitted 405 nm signal. The ratio of $\frac{f_{470\text{ nm}}}{f_{\text{fitted } 405\text{ nm}}}$ was defined as R , and the change of this ratio relative to baseline, ΔR , was calculated as $R - 1$ (where the baseline was defined as $R = 1$, as was the case when 470 nm was scaled to the fitted 405 nm signal). Fluorescence transients were identified using the “findpeaks” function on MATLAB; criteria used to determine what constituted a peak or transient included (1) peaks were at least 0.1 s apart (using the “MinPeakDistance” function variable) and (2) peaks were at least 1.0 R higher than the baseline R value of identified peaks (using the “MinPeakProminence” function variable). Z score was calculated as $\frac{R - \mu}{\sigma}$, where μ is the mean of R and σ the standard deviation of R during the full trial period. Photometry data was downsampled to 30 Hz for binning and synchronization with the behavioral data, which was recorded at 30 frames per second.

Intracranial drug microinjection. To establish the ability of GRAB_{5HT2h} fluorescence to detect 5-HT in vivo, sensor fluorescence was measured while intracranially microinjecting 5-HT (1 μ l per injection, 2 mM; H9523, Sigma-Aldrich) or a 5-HT4R antagonist, RS 23597-190 (2 μ l, 6–10 mM; SML1909, Sigma-Aldrich; 0728, Tocris Bioscience). Both compounds were dissolved in either phosphate-buffered saline (PBS), pH 7.4, or aCSF; controls consisted of injecting the same volume of PBS or aCSF alone. Mice were deeply anesthetized with isoflurane during all injections. To determine the effects of antagonist injection, photometry signals were collected 5 min after the end of anesthesia, when the mice had recovered from anesthesia and were moving freely in the cage.

Optogenetics. For delivery of light used for optogenetic manipulations of serotonergic fiber activity, ANY-maze software (Stoelting) was used to control fiber-coupled light-emitting diodes (LED; M470F3 or M565F3; Thorlabs). Light from the LED was transmitted via optical fiber cables (200 μ m core diameter, 0.5 NA; Thorlabs) coupled with a 1 \times 1 fiber-optic rotary joint (Doric Lenses). Light was delivered as 10 Hz rectangular pulses, 50% duty cycle (470 nm) for photostimulation experiments, or continuously (565 nm) for photoinhibition experiments. Prior to every session, light power output from the tip of the optical fiber patch cable was calibrated using a power meter (S130C and PM100A; Thorlabs). Light power output was set at 4.8 mW for photostimulation experiments (470 nm) or 4.2 mW for photoinhibition experiments (565 nm), such that 3.3–3.6 mW (105–120 mW/mm² irradiance at 470 nm) or 2.9–3.2 mW (92–105 mW/mm² irradiance at 565 nm) of light was delivered from the tip of the optical fiber cannula to the dorsal surface of lobule VII.

Histology and postfixed tissue imaging. To determine the position of optical fiber cannulas following behavioral experiments, mice were deeply anesthetized with pentobarbital before being transcardially perfused with cold PBS and subsequently with 4% paraformaldehyde (PFA). Brains were harvested, postfixed overnight in 4% PFA solution at 4°C and then dehydrated in 30% sucrose solution at 4°C for 2 d. Each brain was frozen with crushed dry ice and sectioned using a freezing sliding microtome. Coronal or sagittal sections (60 or 80 μ m thickness) were obtained and mounted immediately onto microscope slides to maintain section sequence. Brain sections were imaged with a ZEISS Axio Scan.Z1 slide scanner or ZEISS LSM 700 confocal microscope, to confirm both the presence of fluorescence and proper placement of

optical fibers. Mice found to have incorrect or indeterminate placement of optical fibers, or low fluorescence levels, were excluded from analyses.

Behavior analysis. Behavioral testing commenced within 2–4 weeks post-surgery. All mice were handled for 3–4 d before behavioral testing to allow habituation to experimenter contact and connection to the optical fiber patch cable. Mice were habituated to the experimental room in their home cages for 1–2 h prior to the start of each session.

The elevated zero maze (EZM) consisted of two gray open quadrants (45 lux illumination) and two gray closed quadrants enclosed by 14 cm high gray walls (15 lux illumination). The maze was made of stainless steel and had an outer diameter of 55 cm, a 6-cm-wide platform, and was elevated 60 cm off the floor. Animals were individually placed in the middle of an open quadrant at the start of each trial. Each EZM trial lasted for 5 min (fiber photometry) or 10 min (optogenetics). The EZM apparatus was wiped clean with 70% ethanol and allowed to dry completely prior to each trial. Top-view video recordings were made using an ANY-maze USB camera with varifocal lens (Stoelting). ANY-maze software was used to record and track mouse behavior. Trials where mice fell off the EZM or were immobile in the open quadrants for longer than 2 min after the start of the trial, or where the implanted optical fiber cannula detached during the trial, were excluded from analysis of standard EZM behavior. Trials where mice fell off the EZM instead were separately analyzed for their anxiogenic response to falling.

Statistics. All statistical analyses were performed using GraphPad Prism 9. All statistical tests used assumed a nonparametric distribution unless otherwise stated. For pairwise comparisons (within-subject), Wilcoxon signed rank test was used. For comparisons between two groups (between-subject), Mann-Whitney U test was used. Pearson's r test was used for correlation analyses after testing that datasets were normally distributed. For RS 23597-190 antagonist injection experiments, one-way ANOVA test (paired) was carried out with post hoc Tukey's multiple comparisons after confirming that datasets are normally distributed (D'Agostino and Pearson test and Shapiro-Wilk test). Effect sizes are reported as Cohen's d values with the interpretation of 0–0.2 as no effect, 0.21–0.5 as a small effect, 0.51–0.8 as a moderate effect, and >0.8 as a strong effect. In the text, N refers to the number of mice whereas n refers to the number of events or trials. G*Power 3.1 software was used to estimate sample sizes required based on preliminary experimental data. Detailed statistical results are presented in the figure legends. Data are reported as mean \pm SEM, unless otherwise stated.

Results

The cerebellum is thought to be topographically organized into spatial compartments that may be differentially involved in anxiety behavior (Chin and Augustine, 2023). Godlevsky et al. (2014) identified the posterior vermis as a locus involved in regulating anxiety. More recent work has implicated lobule VII of the vermis: inhibiting molecular layer interneurons (MLIs) within this lobule decreases anxiety-related behavior on the elevated plus maze (Badura et al., 2018), while activation of lobule VII MLIs in male mice increases anxiety behavior on the EZM (Chin and Augustine, 2023). Therefore, we examined the role of 5-HT signaling in cerebellar lobule VII in anxiety behavior.

Measurement of 5-HT levels in the cerebellar cortex

We first measured endogenous 5-HT levels by using a second-generation version of the fluorescent 5-HT sensor, G-protein-coupled Receptor-Activation-Based 5-HT sensor (GRAB_{5HT2h}), that reports on extracellular 5-HT levels with high sensitivity and spatiotemporal resolution (Deng et al., 2024). This sensor was expressed in lobule VII via viral transduction [AAV9-hSyn1-5HT3.5(h-S06)]. After virus injection, two-photon imaging (950 nm excitation) revealed that GRAB_{5HT2h} was found across all three layers of the cerebellar cortex: the granule cell

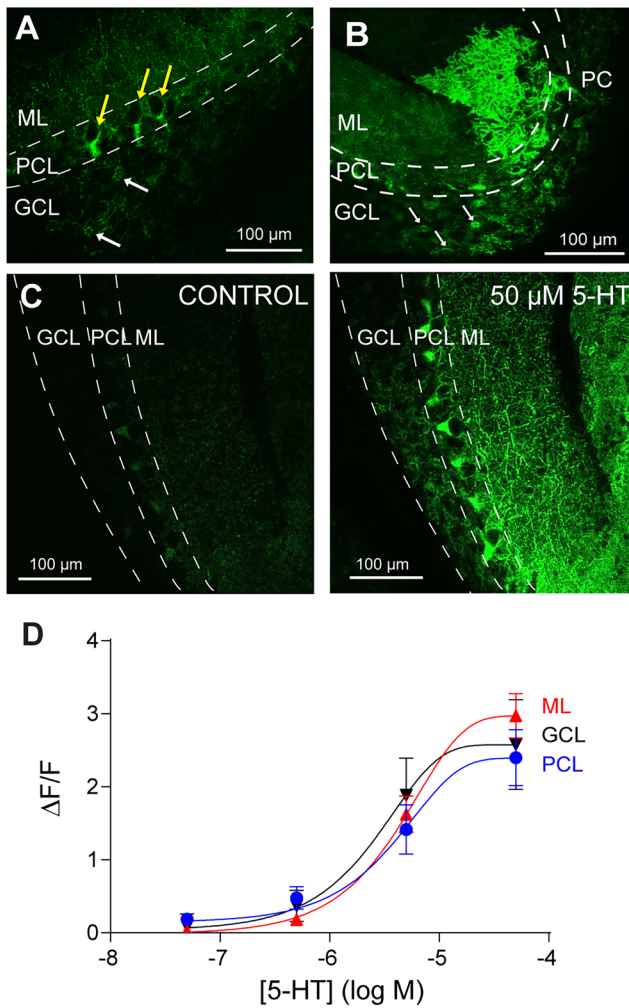


Figure 1. Expression and serotonin responsiveness of GRAB_{5HT2h} in the cerebellar cortex. **A**, GRAB_{5HT2h} expression in neurons within the granule cell layer (GCL), Purkinje cell layer (PCL), and molecular layer (ML) in sagittal cerebellar slices. Yellow arrows indicate basket cell pinneau around Purkinje cell somata and white arrows indicate expression in granule cells. **B**, An example of GRAB_{5HT2h} expression in a Purkinje cell (PC). White arrows indicate expression in granule cells. **C**, GRAB_{5HT2h} fluorescence of cerebellar cortical neurons at the GCL, PCL, and ML in control aCSF (left; control) and in aCSF containing 50 μ M 5-HT (right). **D**, Dose-dependent increases in GRAB_{5HT2h} fluorescence ($\Delta F/F$) in the GCL, ML, and PCL upon treatment with aCSF containing different concentrations of 5-HT. Estimated EC₅₀ values for GRAB_{5HT2h} fluorescence changes in the GCL, PCL, and ML are 48, 69, and 79 mM, respectively. Images were obtained via two-photon imaging. $N = 3$. Data are mean \pm SEM.

layer (GCL), Purkinje cell layer (PCL), and molecular layer (ML; Fig. 1A). The sensor was visible mainly in MLIs, indicated by fluorescent dendrites and fluorescent basket cell pinneau around Purkinje cell somata and axon initial segments (Fig. 1A, yellow arrows). It was also expressed in some granule cells, indicated by fluorescent somata in the GCL (Fig. 1A,B, white arrows). GRAB_{5HT2h} expression in Purkinje cells, evident from the distinctive dendritic arborization of these cells, was rare; sectioning through the entirety of lobule VII revealed only 10–20 fluorescent Purkinje cells per mouse (Fig. 1B). Such sparse expression in Purkinje cells is likely due to our use of the hSyn1 promoter to drive GRAB_{5HT2h} expression: this promoter is known to express transgenes inefficiently in mouse Purkinje cells (Kuhn et al., 2012; Chao et al., 2021).

We tested the ability of GRAB_{5HT2h} to detect 5-HT in the cerebellum by imaging fluorescence in live cerebellar slices from

mice expressing this sensor in lobule VII (Fig. 1C). Bath application of 5-HT increased GRAB_{5HT2h} fluorescence across all three layers of the cerebellar cortex (Fig. 1C), specifically in areas within the ML, basket cell pinneau around Purkinje cells in the PC layer, as well as granule cell somata in the GCL. These increases in sensor fluorescence were highly sensitive to 5-HT concentration, rising as 5-HT concentrations were elevated (Fig. 1D). The relationship between GRAB_{5HT2h} fluorescence and 5-HT concentration was similar across the cerebellum, with half-maximal effective concentrations (EC₅₀) ranging from 48 μ M in the GCL to 79 μ M in the ML; maximal changes in sensor fluorescence were \sim 250% in all layers (Fig. 1D).

After establishing the efficacy of GRAB_{5HT2h} for detecting cerebellar 5-HT, we next used fiber photometry to measure sensor fluorescence in lobule VII in vivo (Fig. 2A). For these experiments, a ratiometric approach was used: the GRAB_{5HT2h} was alternately excited at two wavelengths, one sensitive to 5-HT (470 nm) and a second that is insensitive to 5-HT (405 nm; Fig. 2B). The ratio of green light (525 nm) emitted in response to these two excitation wavelengths created a ratio, R , that was relatively insensitive to photobleaching, movement, and other forms of 5-HT-independent influences on fluorescence emission (Fig. 2B, bottom). To determine whether R reported 5-HT levels, we injected 5-HT into the cerebellar cortex via a cannula; for this experiment, lobule VI was targeted because the small size of lobule VII made it difficult to implant both an injection cannula and an optical fiber. We found that GRAB_{5HT2h} fluorescence ratio increased $12.8\% \pm 1.9$ in response to 5-HT (Fig. 2C; injections indicated by red bars). Control injections of saline had no effect on R (Fig. 2C, blue bars), indicating that GRAB_{5HT2h} readily detects 5-HT within the cerebellum in vivo.

In basal conditions, transient rises in R that lasted for a few seconds were frequently observed (Fig. 2B, bottom). To determine whether these spontaneous signals reflected time-dependent changes in 5-HT levels, we injected a 5-HT₄ receptor antagonist (RS 23597-190, 6–10 mM; Fig. 2D) that blocks GRAB_{5HT2h} sensor responses to 5-HT (Deng et al., 2024). This antagonist decreased the mean amplitude of R (Fig. 2E), as well as the amplitude (Fig. 2F) and frequency (Fig. 2G) of the transient changes in R when compared with control saline injections. Control injections of saline caused smaller decreases in R and in the frequency, but not the amplitude, of transient fluorescence changes. Such effects may have been caused by movement of brain tissue during large injections of saline. When compared with saline injections, GRAB fluorescence was significantly reduced by antagonist injection, indicating that GRAB_{5HT2h} fluorescence is indeed sensitive to 5-HT levels. Collectively, these results demonstrate that fiber photometry measurements of GRAB_{5HT2h} fluorescence readily report cerebellar 5-HT levels. Further, they reveal that 5-HT levels undergo frequent spontaneous fluctuations under basal conditions.

Relationship between 5-HT levels and anxiety behavior

We next examined the relationship between 5-HT levels in lobule VII and anxiety behavior. For this purpose, fiber photometry was used to measure GRAB_{5HT2h} signals in lobule VII, while the EZM was used to monitor anxiety behavior (Fig. 3A). An example of lobule VII GRAB_{5HT2h} signals recorded while a mouse traveled around the EZM is shown in Figure 3B. As is evident in this example, the R of GRAB_{5HT2h} fluorescence emission was higher when the mouse was in the open quadrants (OQ) than when it was in the closed quadrants (CQ). This tendency was more evident when comparing changes in R across experiments

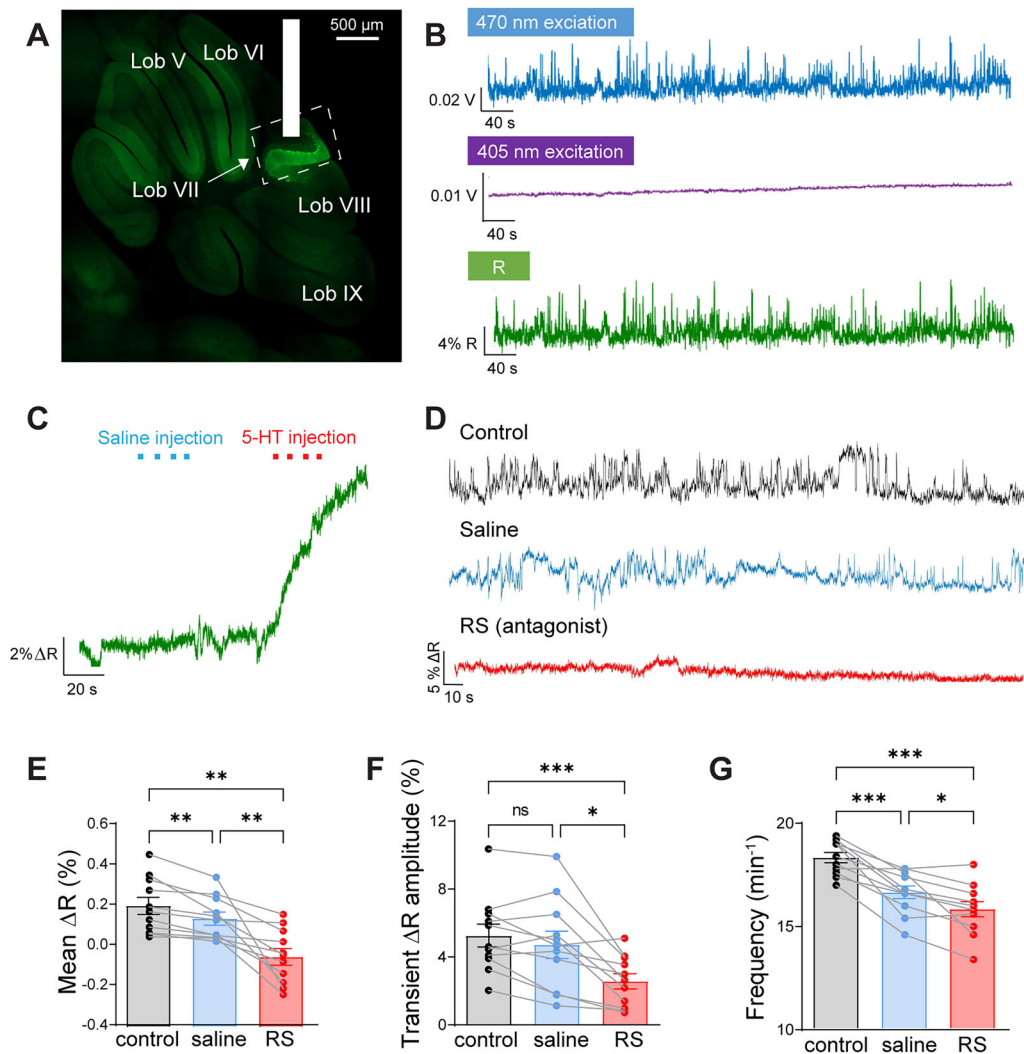


Figure 2. In vivo measurement of GRAB_{5HT2h} responses in the cerebellar cortex. **A**, GRAB_{5HT2h} fluorescence expression in lobule VII (white dashed rectangle) and site of optical fiber implantation (solid white rectangle). **B**, Technique for calculating fluorescence emission ratio, *R*, for GRAB_{5HT2h} signals in lobule VII. Fiber photometry measured GRAB_{5HT2h} fluorescence in a mouse moving around a novel cage. Fluorescence emission produced by excitation at 470 nm (top; 5-HT-dependent) and 405 nm (middle; isosbestic control) were used to calculate ratio, *R*, of GRAB_{5HT2h} (bottom). **C**, Example of *R* signal in lobule VI that did not change upon intracranial injections of saline (blue bars) but increased in response to injections of 5-HT (2 mM; red bars). The volume of each injection was 1 μ l. **D**, Examples of *R* signals measured in control conditions (top), after saline injection (middle), and after injection of 5-HT receptor antagonist RS23597-190 (6–10 mM, bottom). Signals were recorded when mouse was awake from anesthesia and moving around its cage. **E**, Mean ΔR of GRAB_{5HT2h} decreased drastically upon intracranial injection of 5HT4R antagonist (RS) compared with saline injection. $F_{(2,10)} = 16.9$, $p = 0.002^{**}$; saline–control: $F_{(2,10)} = 16.94$, $p = 0.002^{**}$, $d = -0.507$; RS–control: $p = 0.004^{**}$, $d = -1.83$; RS–saline: $p = 0.008^{**}$, $d = -1.54$. **F**, Maximum amplitude of transient changes in *R* significantly decreased after RS injection, but not after saline injection; $F_{(2,10)} = 17.3$, $p < 0.001^{***}$; saline–control: $p = 0.263$, $d = -0.218$; RS–control: $p < 0.001^{***}$, $d = -1.42$; RS–saline: $p = 0.012^*$, $d = -0.998$. **G**, Frequency of transient changes in *R* decreased significantly after RS injection, as well as after injection of control saline; $F_{(2,10)} = 34.3$, $p < 0.001^{***}$, saline–control: $p < 0.001^{***}$, $d = -1.84$; RS–control: $p < 0.001^{***}$, $d = -2.40$; RS–saline: $p = 0.023^*$, $d = -0.719$. One-way ANOVA (paired; parametric distribution), Tukey’s multiple-comparisons post hoc test. $N = 11$. Bars in **E–G** show mean values, while error bars indicate ± 1 SEM. Points indicate values for individual experiments.

(Fig. 3C): the mean change in *R* (ΔR), compared with an initial baseline where *R* was defined as 1) was significantly higher when mice were in the OQ. However, numerous transient changes in *R* are evident in Figure 3B even while the mouse remained within the CQ. Indeed, there were no significant differences in the amplitude (Fig. 3D), frequency (Fig. 3E), or half-width (Fig. 3F) of the transient signals between the OQ and the CQ. Thus, the changes in *R* observed in the two quadrants were associated with slow shifts in baseline, rather than the more rapid and transient increases in *R*. Such increases in baseline *R* were often observed in mice when they entered the OQs. In the example in Figure 3B, the increase in baseline fluorescence plateaued during the time when this mouse was in the OQ and reverted back to baseline levels when the mouse retreated into

the CQs. Similar changes in basal 5-HT levels when mice entered and exited the OQs were observed in most, but not all, mice (10 out of 16). In the other six mice, three displayed no changes in 5-HT levels, while transient increases in *R* were observed 3–5 s before the other three mice entered the OQ, but *R* then decreased back to baseline while these mice were in the OQ. Our subsequent analysis includes data from all 16 mice.

Kinetics of 5-HT changes in lobule VII

Simply parsing GRAB_{5HT2h} fluorescence into times that mice were in either the OQ or the CQ necessarily will include times involving other behaviors that may not be directly related to anxiety, such as locomotion within a quadrant. To discern the changes in *R* specifically associated with anxiety, we focused on

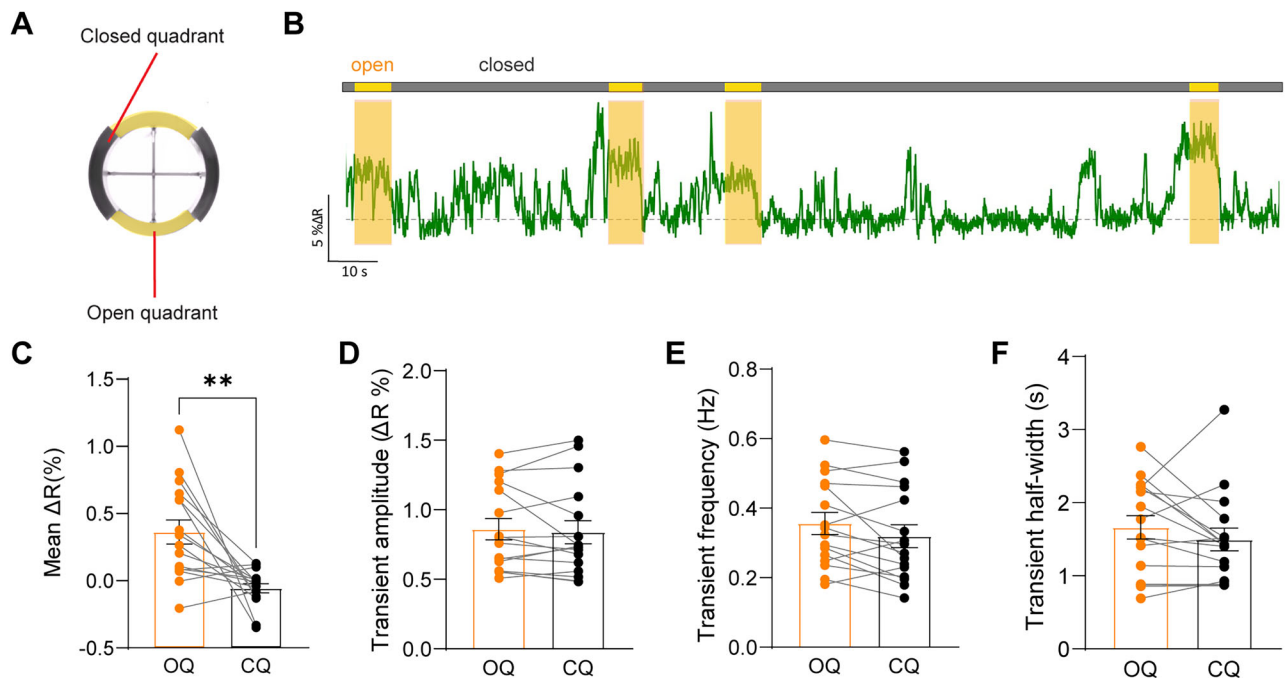


Figure 3. Endogenous 5-HT levels inversely correlate with anxiety state. **A**, Top view of the elevated zero maze (EZM), showing open quadrants (OQ) and closed quadrants (CQ). **B**, Example of R measurement in lobule VII while mouse was in the EZM. R was higher when mouse was in OQs (orange bars). **C**, Mean ΔR was higher when mice were in OQs compared with CQs; $W = 116$, $p = 0.001^{**}$, $d = 1.5$. **D–F**, Mean amplitude, frequency, and half-width of transient changes in R in lobule VII did not significantly differ when mice were in OQs and CQs; p values for **D–F**: 0.9; 0.05; 0.19; Cohen's d values: 0.07, 0.28, 0.26. Wilcoxon signed rank test; $N = 16$. Bars in **C–F** show mean values, while error bars indicate ± 1 SEM. Points indicate values for individual experiments.

5-HT levels when mice either entered the OQs (approach) or when they exited the OQs and entered the CQs (retreat). Measurements across animals were standardized by calculating the Z scores of GRAB_{5HT2h} fluorescence R values. Z scores increased during the time that mice approached the OQs (Fig. 4A), with the mean value of Z scores across experiments increasing significantly (Fig. 4B). Further, Z scores decreased as mice retreated into the CQs (Fig. 4C), with the mean reduction across experiments again being statistically significant (Fig. 4D).

To determine the precise timing of these changes in R , relative to the time of OQ entries and exits, a bilevel waveform was interpolated to the signals (Fig. 4A,C, dashed lines). The rise time was defined as the time when the fitted waveform increased from 10 to 90% of its maximum, while the fall time defined the time when the fitted waveform decreased from 90 to 10% of its maximum value. Mean Z scores increased 3.4 s before mice entered the OQs, with a rise time (10–90%) of 3.3 s (Fig. 4A). Similarly, mean Z scores decreased 0.4 s before mice retreated into the CQs, with a fall time (90–10%) that was also 3.3 s (Fig. 4C). In summary, this kinetic analysis revealed that 5-HT levels started to increase as mice approached the OQs, prior to entry, and began to decrease prior to their exit from the OQs.

Higher 5-HT levels in lobule VII are associated with more and longer OQ visits

The EZM is an approach–avoidance test that capitalizes on the conflict between two opposing behavioral forces: avoiding the aversive environment of the OQ versus the innate exploratory drives of mice (Calhoun and Tye, 2015; Tovote et al., 2015). Thus, when mice approach OQs, they should be less anxious, allowing their exploratory drive to overcome the aversiveness of the OQ. By considering all OQ entry events within a trial

and across multiple trials and animals, we found that OQ entry events where Z scores increased above baseline occurred more frequently ($n = 300$; Fig. 4E, top) than OQ events where Z scores decreased ($n = 180$; Fig. 4E, bottom). This is consistent with the possibility that higher 5-HT levels reflect a low-anxiety state.

If higher 5-HT levels are associated with lower anxiety levels, then 5-HT levels should also positively correlate with the duration of OQ entries. Indeed, out of 480 OQ visits across all trials in all mice, the mean duration of time spent in the OQ was significantly higher when Z scores increased than when Z scores decreased (Fig. 4F). This indicates that lower 5-HT levels in lobule VII are associated with shorter OQ visits (higher anxiety), and higher 5-HT levels are associated with longer OQ visits (lower anxiety). Thus, lobule VII 5-HT levels inversely correlate with the anxiety state of mice.

Mouse falling decreases lobule VII 5-HT levels

In the course of our experiments, mice occasionally fell off the EZM. Because this represented a highly aversive situation, we asked whether lobule VII 5-HT levels were lower in trials with falls. In seven animals that experienced a fall, plots of Z score over time were analyzed before falling, during the fall (while they were hanging onto the optical fiber), and after the fall, when mice were placed back onto the middle of the OQ (Fig. 5A). In six out of seven cases, 5-HT levels decreased during a fall; overall, the mean reduction in R across experiments was statistically significant (Fig. 5B). This provides another indication that 5-HT levels inversely correlate with anxiety levels.

The latency to retreat into the CQ following a fall varied between mice (Fig. 5A). This allowed us to ask whether this variability was associated with 5-HT levels. Z score values for R after a fall positively correlated with the latency for retreat into the CQ

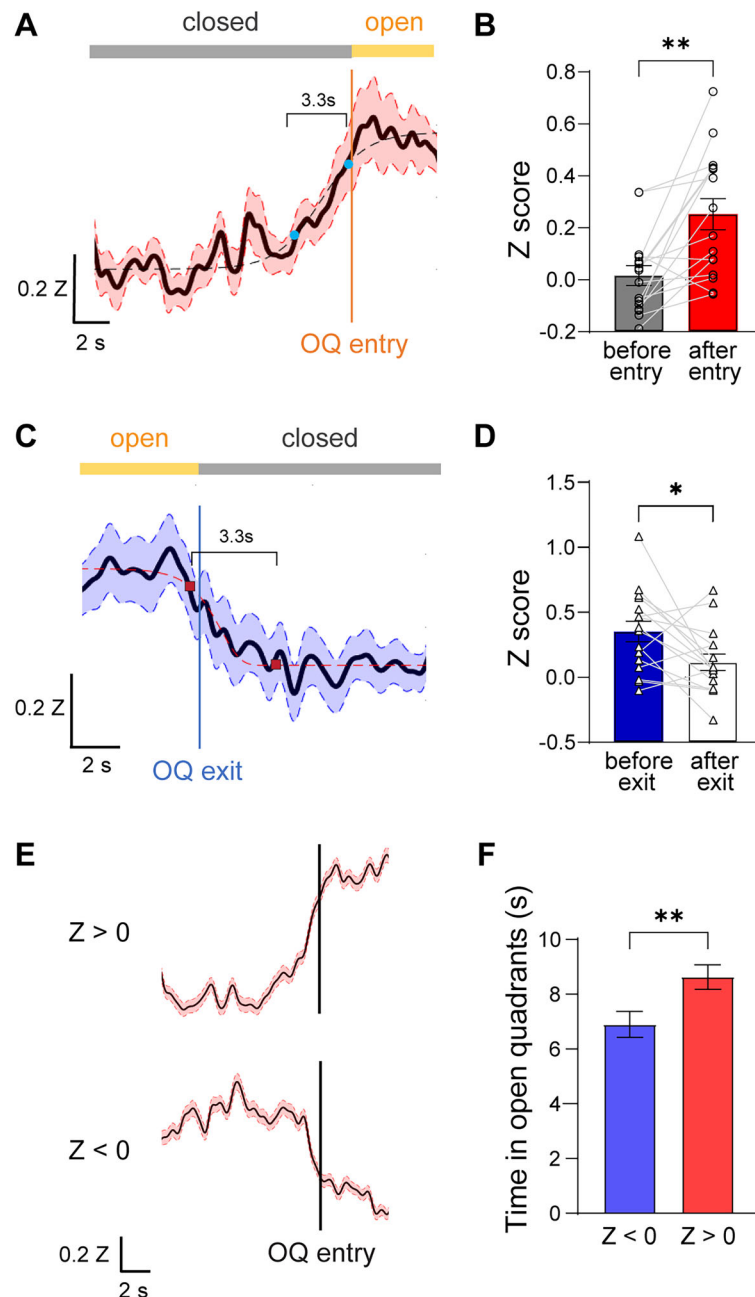


Figure 4. 5-HT levels change during transitions between quadrants. **A, C**, Time course of mean Z scores (black) of lobule VII *R* values, aligned to times when mice (**A**) entered OQs (orange vertical line) and (**C**) exited OQ (blue vertical line). Shaded areas indicate ± 1 SEM. Dashed lines indicate bilevel waveforms fit to data. Blue circles in **A** and red squares in **C** show times for 10 and 90% completion of rise or fall of bilevel waveforms, with brackets indicating rise and fall times. **B**, Z scores significantly increased when mice entered the OQs (measured 10 s before entry and 5 s after entry). Wilcoxon signed rank test; $W = 118$, $p = 0.001^{**}$, $d = 1.2$. **D**, Z scores significantly decreased when mice exited the OQs (measured 5 s before exit and 10 s after exit). $W = -82$, $p = 0.034^*$, $d = -0.83$. **E**, Average time course of GRAB_{5HT2h} signals when $Z > 0$ or $Z < 0$ during OQ entries. $n = 300$ ($Z > 0$) and 180 ($Z < 0$). **F**, Mean duration spent per OQ entry was higher for events where mean Z is higher than 0, compared with when mean Z decreases were below 0 (Mann–Whitney test; $U = 22,596$, $p = 0.003^{**}$, $d = 0.24$); $n = 180$ ($Z < 0$) and 300 ($Z > 0$).

(Fig. 5C). This indicates that, after a fall, mice retreated into the CQ faster—indicating higher anxiety—when 5-HT levels in lobule VII were lower and retreated more slowly when 5-HT levels were high. This provides one final indication of the inverse relationship between 5-HT levels in lobule VII and anxiety behavior.

In summary, our fiber photometry experiments demonstrate that physiological 5-HT levels in lobule VII varied during anxiety states. Lobule VII 5-HT levels increased when mice were less anxious, namely, before they entered the OQs and when they spent more time in the OQs. Serotonin levels decreased when mice were more anxious: when they retreated to the CQs, when they

spent less time in the OQs, and when they fell off the EZM. Therefore, our results reveal that lobule VII 5-HT levels are inversely related to the anxiety state of mice.

Increasing 5-HT input decreases anxiety

The results described above indicate a relationship between lobule VII 5-HT levels and anxiety behavior but do not establish the cause of this relationship. The fact that changes in 5-HT levels precede overt changes in anxiety behavior (Fig. 4A,C) suggests the hypothesis that 5-HT levels regulate anxiety behavior. To test this hypothesis, we used optogenetics to manipulate the activity of

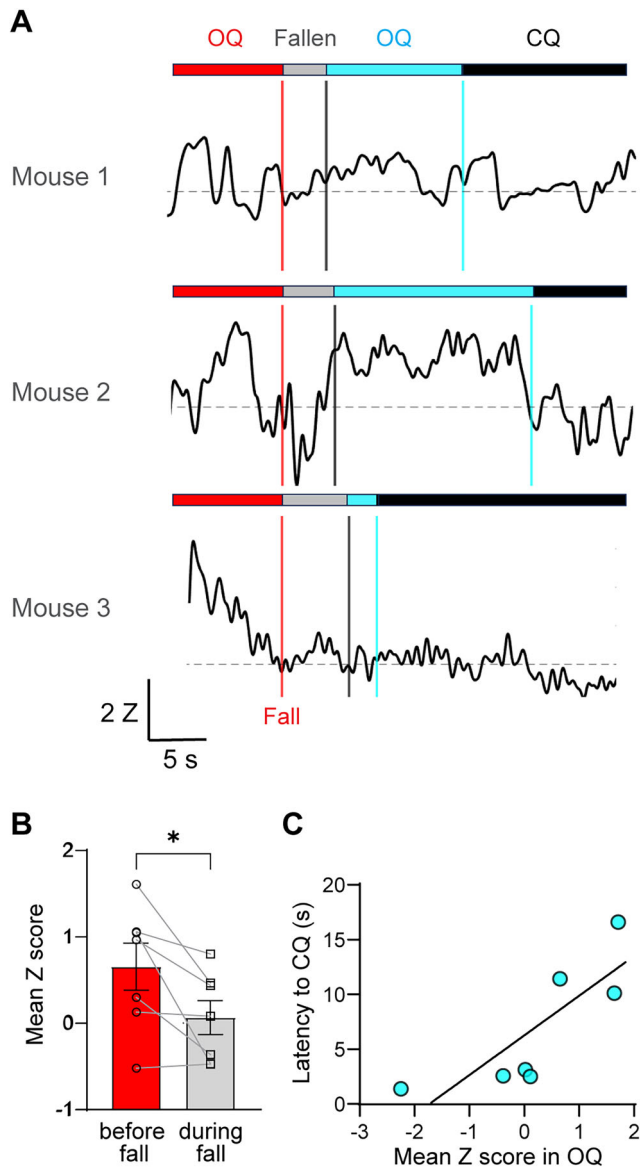


Figure 5. 5-HT levels decrease when mice fall from the EZM. **A**, Three examples of Z scores of lobule VII GRAB_{5HT2A} signals, aligned to the time mice fell off the EZM (red vertical lines). Black vertical lines indicate times when mice were placed back onto the OQ, while cyan vertical lines indicate times when mice retreated into the CQ. After placement back onto the OQ, mice retreated back into the CQs. Horizontal dashed lines indicate $Z = 0$. **B**, Mean Z score decreased significantly during falls (comparing 10 s before fall and to the full duration of falls, which ranged from 4 to 6 s). Wilcoxon signed rank test; $W = -26$, $p = 0.031^*$, $d = -0.94$. Bars show mean values, while error bars indicate ± 1 SEM. Points indicate values for individual experiments. **C**, Relationship between mean Z scores after falling, when mice were placed back onto the OQ, and time required to retreat to CQ ($r = 0.807$, $p = 0.03$; Pearson's correlation test; $N = 7$).

serotonergic terminals innervating lobule VII while monitoring the effects of these changes in 5-HT input on anxiety behavior.

We first examined the structure and distribution of these inputs in mice expressing YFP-tagged ChR2 in serotonergic neurons. For this purpose, ePet-Cre mice (Scott et al., 2005) were cross-bred with Ai32 mice (Madisen et al., 2012) to yield expression of YFP-tagged ChR2 in serotonergic neurons. The ePet-Cre mouse line is reported to have high specificity for targeting raphe 5-HT neurons (Cardozo Pinto et al., 2019). However, the penetrance of this line is $<100\%$, so that not all serotonergic neurons in the double-transgenic mice (ePet-ChR2 mice) will express ChR2. YFP fluorescence was used to visualize serotonergic cells,

projections, and terminals in fixed coronal sections of the ePet-ChR2 mice. Cell bodies of neurons expressing YFP were mainly found in the dorsal raphe (Fig. 6A), median raphe, and the medullary raphe; these locations are well-known to contain serotonergic neurons (Scott et al., 2005; Ohmura et al., 2014; Hernandez-Vazquez et al., 2019), confirming our genetic targeting strategy. YFP-labeled 5-HT axon terminals were widely observed throughout the cerebellum, in both the cerebellar nuclei (CN; Fig. 6B) and the cerebellar cortex, including lobule VII (Fig. 6C–G). These terminals—indicated by white triangles in Figure 6C—were observed within all three layers of the cerebellar cortex: PCL (Fig. 6C), GCL (Fig. 6D), and ML (Fig. 6G). Although 5-HT fibers were difficult to identify, because their dim YFP fluorescence was difficult to discern among background autofluorescence, they were observed (white arrows) within the GCL (Fig. 6E) and the ML (Fig. 6F,G). Our observations coincide with early demonstrations of 5-HT fibers throughout the entire cerebellar cortex (including lobule VII) and within each of the three layers of the cerebellar cortex (Takeuchi et al., 1982; Bishop and Ho, 1985; Triarhou and Ghetti, 1991; Longley et al., 2021). In summary, lobule VII of ePet-ChR2 mice receives 5-HT afferents that express ChR2.

We photostimulated these afferents in mice that were placed on the EZM for a total of 10 min. After allowing 2 min to record basal behavior, blue light (470 nm) was delivered to lobule VII between the 2nd and 4th minutes. Photostimulation of 5-HT axons in lobule VII caused mice to spend more time in the OQs of the EZM (Fig. 7A1). This effect was not observed in control mice that did not express ChR2 in their 5-HT neurons (Fig. 7B1), thereby excluding the possibility that the effect was caused by heating or other unintended consequences of illuminating lobule VII. Neither mouse mobility (Fig. 7A2, B2) nor distance traveled (Fig. 7A3, B3) changed significantly during the time of light delivery. This indicates that the increased time spent in OQs upon activating 5-HT input did not arise from changes in locomotor activity but instead was likely caused by a decrease in anxiety levels in photostimulated mice. The number of entries into OQs also appeared to increase upon photostimulating 5-HT axons in lobule VII, though this change was not statistically significant (Fig. 7A4). Light delivery did not significantly affect the number of entries into OQs in control mice (Fig. 7B4).

One confound in interpreting post-photostimulation behavior is that habituation to the EZM caused both ePet-ChR2 (Fig. 7A2) and control (Fig. 7B2) mice to move less over time. To account for such habituation-related reductions in locomotion, the time spent in OQs (Fig. 7A1, B1) was normalized by dividing by the total time that mice were mobile (Fig. 7A2, B2). This transform showed that photostimulation of 5-HT axons increased the fraction of time mice were mobile within the OQs (Fig. 7A5), an effect that again was not observed in control mice (Fig. 7B5). Further, the effects of photostimulation were maintained until the end of the 10-min-long trial. The observations that mice spent both more time (Fig. 7A1) and a greater portion of their total exploration time (Fig. 7A5) in the aversive OQs, rather than the safer CQs, indicates that photostimulation of lobule VII 5-HT axons was anxiolytic. Furthermore, even after habituation decreased the exploratory drives of ePet-ChR2 mice, photostimulation still caused them to occupy OQs for a greater fraction of the time that they were mobile. Taken together, our results showed that photostimulating 5-HT axons in lobule VII of male mice yielded anxiolytic behavior, therefore indicating that activating 5-HT input is sufficient to decrease anxiety.

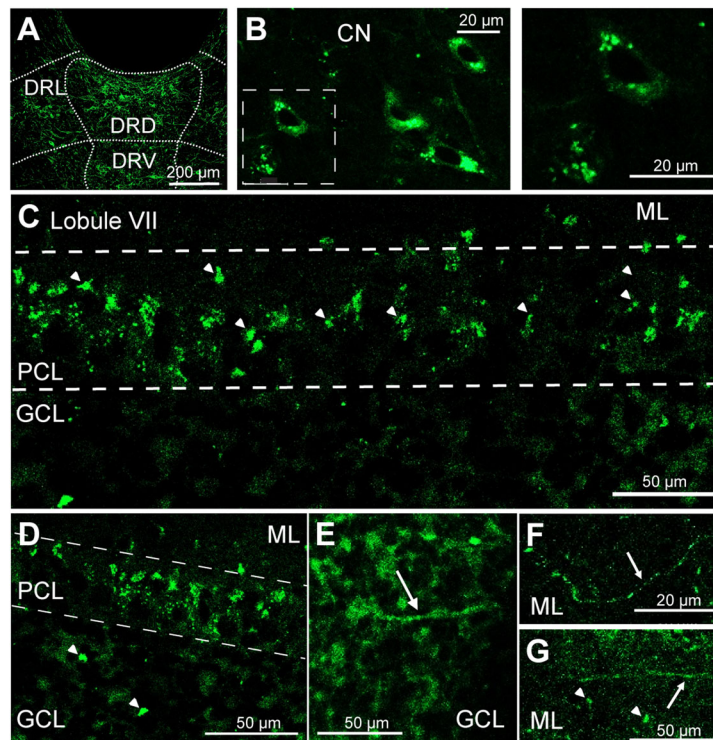


Figure 6. ChR2 expression in serotonergic neurons of double-transgenic mice. **A**, Fluorescence of YFP-tagged ChR2 in serotonergic neurons in the dorsal raphe nucleus. DRD, dorsal raphe nucleus, dorsal part; DRL, dorsal raphe nucleus, lateral part; DRV, dorsal raphe nucleus, ventral part. **B**, ChR2 expression in synaptic terminals of 5-HT neurons in medial cerebellar nucleus; similar expression was observed throughout all cerebellar nuclei (CN). **C–G**, ChR2 expression in serotonergic terminals (arrowheads) in lobule VII of cerebellar cortex. Expression was observed in Purkinje cell layer (PCL), granule cell layer (GCL), and molecular layer (ML). White arrows indicate putative 5-HT fibers in the GCL (**E**) and ML (**F** and **G**) of lobule VII.

Decreasing 5-HT input increases anxiety

We next asked whether optogenetic reduction of the activity of 5-HT input to the cerebellum had any effect on anxiety behavior. For this purpose, ePet-Cre mice were mated with Ai35 mice (Madisen et al., 2012) to yield expression of YFP-tagged Arch in serotonergic neurons (ePet-Arch mice). These double-transgenic mice allowed us to determine the behavioral consequences of photoinhibiting the 5-HT afferents of lobule VII. Upon photoinhibition (565 nm light), mice spent significantly less time in the OQs of the EZM (Fig. 8A1). The number of times that mice entered the OQs also significantly decreased upon photoinhibition of 5-HT axons in lobule VII (Fig. 8A4). These effects were not observed in control mice that did not express Arch in 5-HT neurons (Fig. 8B1,B4), indicating that the reduction in OQ occupancy following illumination of ePet-Arch mice was specifically caused by inhibiting the activity of 5-HT input to the cerebellum. Further, neither the mobility (Fig. 8A2,B2) nor the distance traveled by mice (Fig. 8A3,B3) were significantly affected during light delivery. This indicates that the decrease in time spent in the OQs was not caused by changes in locomotor ability of the mice but instead was a genuine increase in anxiety levels upon inhibiting 5-HT input.

To account for the effects of habituation (Fig. 8A2,B2), the time spent in the OQs was again normalized by dividing by the total amount of time that the mice were mobile. This analysis indicated that photoinhibition caused mice to spend a significantly lower fraction of the time that they were mobile in the OQs (Fig. 8A5), and this effect continued until the end of the trial (Fig. 8A5). These effects were not observed in control mice (Fig. 8B5). Collectively, our results indicate that photoinhibition of 5-HT axons in lobule VII led to an anxiogenic effect on EZM behavior, while

photostimulation of these axons had the opposite effect. We therefore conclude that activity in the 5-HT input into lobule VII is both necessary and sufficient to modulate anxiety behavior in male mice.

Discussion

Our results reveal that regulation of anxiety behavior by the cerebellum of male mice is mediated, at least in part, by the actions of 5-HT in lobule VII. The use of a highly sensitive and specific 5-HT fluorescent sensor (Deng et al., 2024) revealed that endogenous 5-HT levels in lobule VII inversely correlate with anxiety states, as measured by the EZM. 5-HT levels were higher when mice were less anxious, specifically when they approached the OQ or when they spent more time in the OQ. On the other hand, 5-HT levels were lower when mice were more anxious, specifically when they retreated into the CQ, spent less time in the OQ, or fell off the EZM. Further, our optogenetic manipulations of serotonergic neuron activity complemented these measurements of 5-HT levels by demonstrating that changes in lobule VII 5-HT levels are both necessary and sufficient for cerebellar regulation of anxiety behavior. We found that increasing 5-HT input into lobule VII decreased anxiety, while decreasing 5-HT input into lobule VII robustly increased anxiety levels. Collectively, our findings satisfy the “show it, move it, block it” criteria for establishing causality (Steinhardt, 2006) and, thereby, demonstrate that lobule VII 5-HT inputs regulate anxiety behavior.

Because of the well-established role of the cerebellum in regulating motor function, it was important for us to discern whether our 5-HT measurements and manipulations of serotonergic neuron activity reflected changes in anxiety behavior or stemmed from alterations in motor functions. Our fiber photometry measurements revealed that 5-HT levels in lobule VII

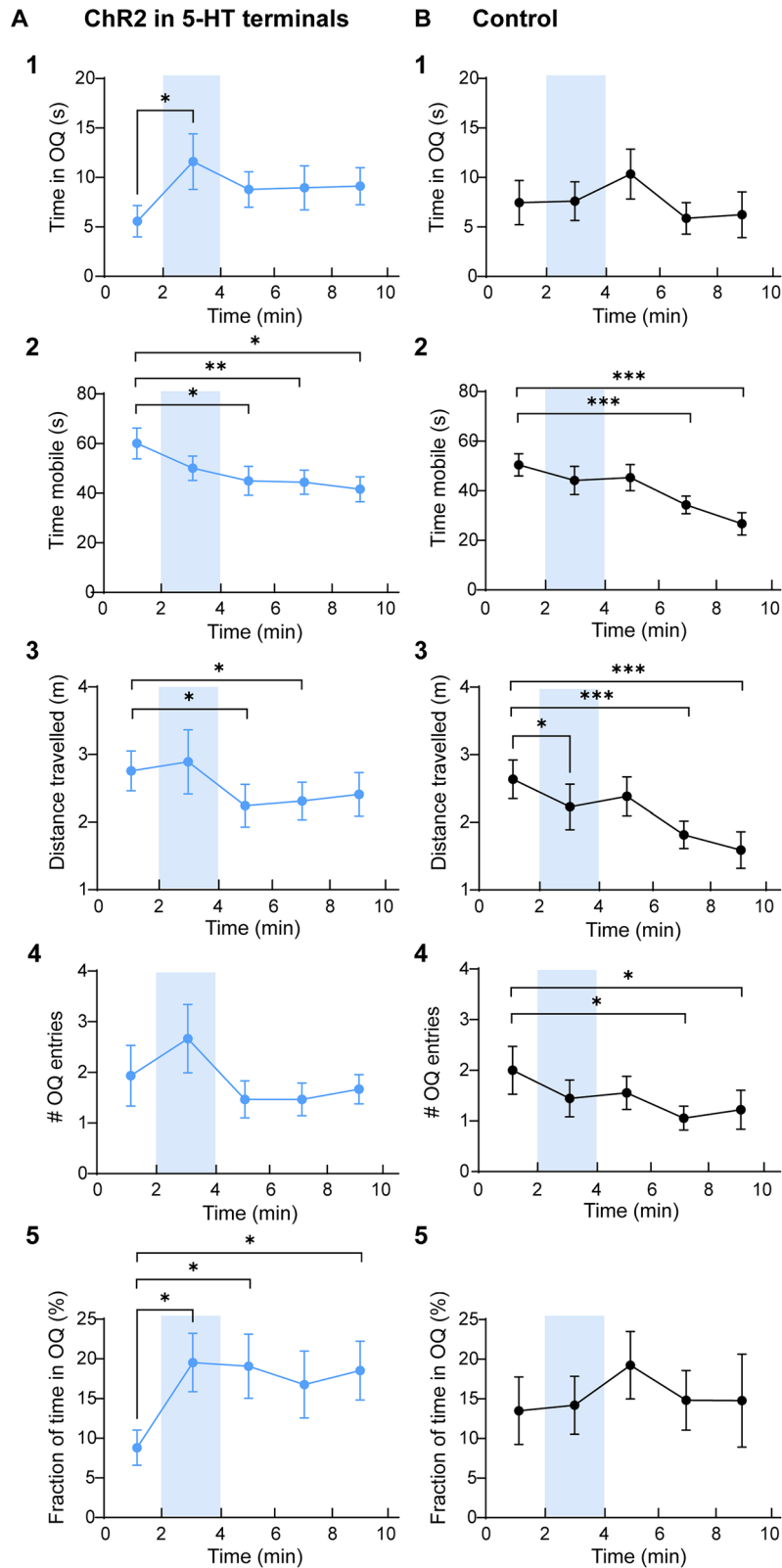


Figure 7. Anxiolytic behavior produced by optogenetic photostimulation of lobule VII 5-HT axons. Mice were placed on the EZM, while light (470 nm) was delivered to lobule VII during time indicated by blue bars. In column **A**, light was delivered to mice expressing Chr2 in 5-HT axons, while in column **B**, it was delivered to control mice not expressing Chr2. **A1**, Photostimulation significantly increased time spent in open quadrants (OQ; $p = 0.03^*$, $d = 0.68$) but had no immediate effect on mobility (**A2**), distance traveled (**A3**), or number of entries into the OQs (**A4**). In **A2–3**, habituation to the EZM led to mice moving less over time; asterisks indicate significant p values: 0.022^* , 0.003^{***} , 0.03^* (**A2**) and 0.41^* , 0.48^* (**A3**). **A5**, Photostimulation increased fraction of time spent in OQ and remained elevated until end of the trial. Asterisks indicate significant p values: 0.02^* , 0.01^* , 0.48^* . **B1–5**, Light delivery to control mice did not significantly affect the indicated behavioral parameters, aside from a decrease in distance traveled (**B3**); $p = 0.021^*$, $d = -0.3$. Similarly, habituation to the EZM led to mice moving less over time (**B2–4**). Asterisks indicate significant p values: 0.001^{***} , 0.001^{***} (**B2**), 0.021^* , 0.001^{***} , 0.001^{***} (**B3**), 0.034^* , 0.045^* (**B4**). Wilcoxon signed rank test; points represent mean values and error bars indicate ± 1 SEM. Sample sizes were 15 (**A**) and 18 (**B**).

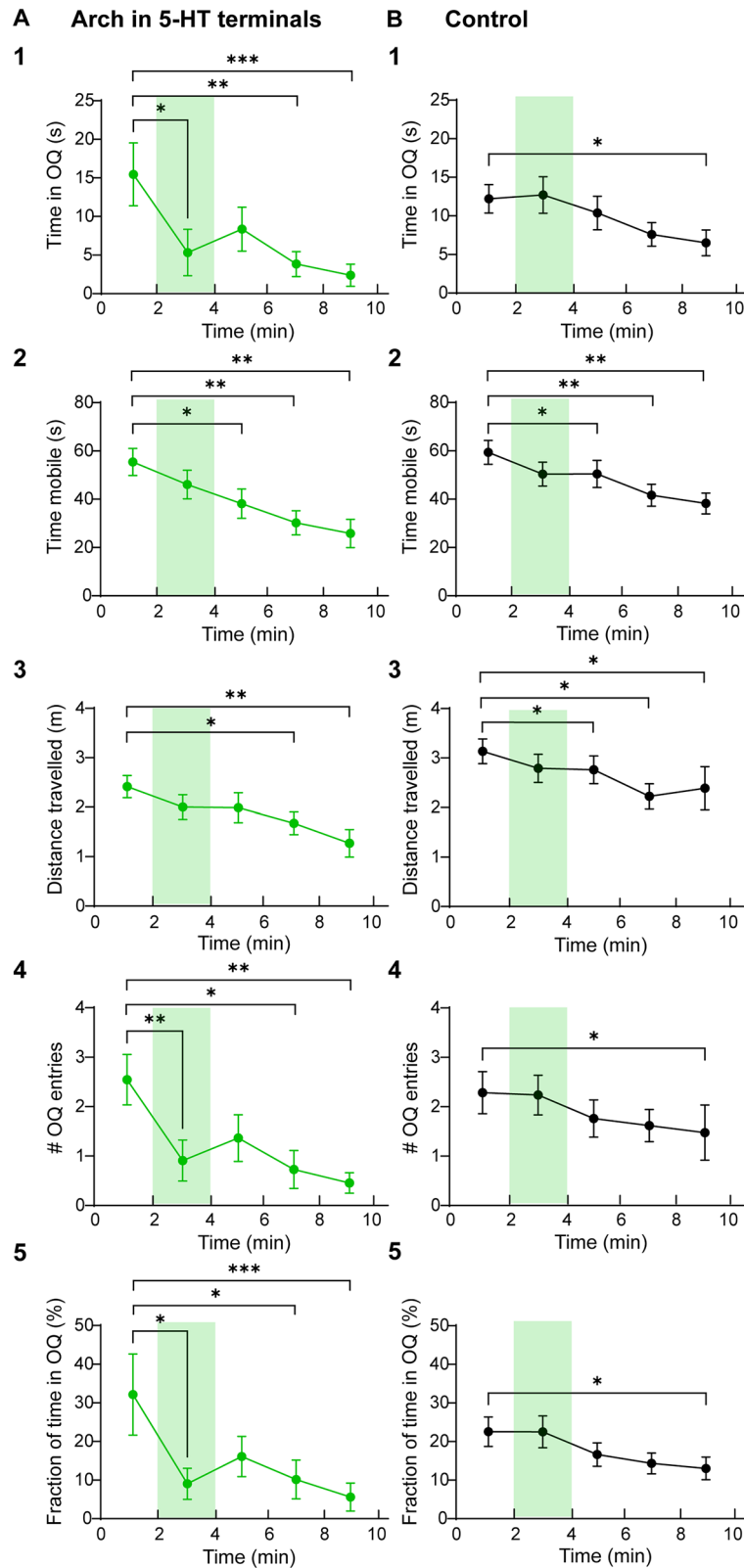


Figure 8. Anxiogenic behavior produced by optogenetic photoinhibition of lobule VII 5-HT axons. Mice were placed on the EZM, while light (565 nm) was delivered to lobule VII during time indicated by green bars. In column **(A)**, light was delivered to mice expressing Arch in 5-HT axons, while in column **(B)** it was delivered to control mice not expressing Arch. **A1**, Photoinhibition of lobule VII 5-HT axons significantly decreased time spent in the open quadrants (OQ; *p* values: 0.032*, 0.175, 0.002**, <0.001***) and **(A4)** number of entries into the OQs (*p* values: 0.008**, 0.1, 0.012*, 0.002**), yet had no immediate effect on **(A2)** mobility or **(A3)** distance traveled in male mice. In **A2–3**, habituation to the EZM led to mice moving less over time. Asterisks indicate *p* values: **(A2)** 0.032*, 0.002**, 0.003**, and **(A3)** 0.024*, 0.01**. **A5**, Fraction of time in OQ significantly decreased upon photoinhibition of lobule VII 5-HT axons (*p* values: 0.032*, 0.24, 0.032*, <0.001***). **B**, Light delivery to control mice did not significantly affect the indicated behaviors, although habituation to EZM led to mice moving less over time **(B2–3)**. Asterisks indicate *p* values: **(B2)** 0.042*, 0.007**, 0.003**, and **(B3)** 0.018*, 0.011*, 0.024*. Wilcoxon signed rank test; points represent mean values and error bars indicate ±1 SEM. Sample sizes were 11 **(A)** and 21 **(B)**.

increased seconds before mice approached the OQs of the EZM and conversely started decreasing before mice retreated into the CQs. The opposite directions of these changes indicated that they were unlikely to reflect the motor component of these behaviors: if 5-HT changes purely reflected movement across OQ-CQ borders, then they should change in the same direction whether entering or exiting a quadrant. Thus, the opposing changes in 5-HT levels during approaches and retreats likely reflected the positive and negative valence associated with each anxiety-related behavior. Additionally, optogenetic manipulation of 5-HT inputs in lobule VII did not produce any gross motor impairment, because mice were able to walk, turn around, and rear properly. The mobility of, and distance traveled by, these mice on the EZM—during both optogenetic activation and inhibition of lobule VII 5-HT fibers—were also comparable with those of control mice. This indicates that manipulation of 5-HT input into lobule VII directly perturbed the anxiety circuit, rather than affecting circuitry involved in motor function. This conclusion is consistent with our observations that directly increasing and decreasing 5-HT input into lobule VII bidirectionally altered anxiety behavior on the EZM. Therefore, changes in 5-HT levels and behavioral output on the EZM likely reflect changes in anxiety behavior rather than motor behavior.

An intriguing observation from our optogenetic experiments was that the anxiolytic and anxiogenic effects of photostimulation and photoinhibition of 5-HT axons in lobule VII seemed to persist well beyond the time of light application (Figs. 7, 8). A possible explanation is that photostimulation and/or photoinhibition of 5-HT axons induced circuit plasticity within lobule VII. Consistent with this possibility, 5-HT_{2a}R modulation of synaptic plasticity at the parallel fiber→Purkinje cell synapse has been reported (Oostland et al., 2014).

A common caveat of *in vivo* photostimulation is that unintended activation of axon collaterals of a photostimulated neuron—caused by backpropagation of action potentials—may cause side effects. 5-HT neurons are known to broadly project collaterals to multiple brain regions, possibly for coordinated regulation of multiple brain regions with related functions (Waselus et al., 2011; Wong et al., 2021). Thus, it is possible that axon collaterals of 5-HT neurons projecting to other brain regions were also activated during photostimulation and caused the observed anxiolytic behavior. We believe that this explanation is unlikely, because activating 5-HT input in other brain areas typically yields anxiogenic effects (Andrade et al., 2013; Ohmura et al., 2014; Teissier et al., 2015; Marcinkiewicz et al., 2016; Abela et al., 2020), which is the opposite of what we observed. Therefore, photostimulation of axon collaterals of 5-HT neurons is unlikely to account for our results, though it could explain why photostimulation of cerebellar 5-HT axons yielded only a mild anxiolytic effect. Additionally, our photoinhibition experiments—which avoided action potential back propagation—yielded complementary results. Thus, our findings support a role for 5-HT input into lobule VII on anxiety behavior. On the other hand, we are unable to exclude the possible involvement of other neurotransmitters, such as glutamate, that may be coreleased during photostimulation of 5-HT inputs (Sengupta et al., 2017; Cardozo Pinto et al., 2019). Because of the coherence of our 5-HT measurements and the results of optogenetic manipulation of 5-HT axon activity, the most parsimonious interpretation is that 5-HT input into lobule VII is indeed involved in regulating anxiety behavior. Specifically, all of our experiments are consistent with the conclusion that 5-HT input into lobule VII produces an anxiolytic effect.

Early studies of the cerebellar 5-HT system postulated that the modulatory effects of 5-HT on cerebellar neurons likely regulate sensorimotor-related functions (Mitoma et al., 1994; Mendlin et al., 1996). However, recent advances in our understanding of the role of the cerebellum in a plethora of non-motor functions have led to findings that cerebellar neuromodulators may also be involved in non-motor functions, such as emotional memory and social behavior (Fernandes et al., 2017; Cutando et al., 2022). Recently, Kim et al. (2021) identified a role for 5-HT in the cerebellar nuclei in regulating stress-induced dystonia, alluding to a possible role for the cerebellar 5-HT system in modulating aversive behaviors. Our findings provide the first line of evidence for a role for 5-HT input to the cerebellar cortex in regulating aversive behavior, specifically anxiety.

Our results also provide further evidence supporting a role for lobule VII as an anxiety locus in the cerebellum. The first hints of the role of lobule VII as a specific locus in regulating anxiety behavior came from the incidental observations of Badura et al. (2018) that inhibition of lobule VII MLIs decreases anxiety. Our previous experiments demonstrated that activation of lobule VII MLIs of male mice increases anxiety (Chin and Augustine, 2023), thereby establishing that lobule VII MLI activity bidirectionally regulates anxiety behavior. The cellular targets of 5-HT within lobule VII remain to be determined. Although previous work indicated that 5-HT does not directly regulate MLI activity (Dieudonné and Dumoulin, 2000), this may need to be revisited in light of recent findings that neuromodulator receptors are differentially expressed in different parts of the cerebellar cortex (Canton-Josh et al., 2022; Cutando et al., 2022). Clear effects of 5-HT on the activity of PCs (Li et al., 1993; Saitow et al., 2013), parallel fiber-PC synapses (Maura et al., 1988; Oostland et al., 2014; Fleming and Hull, 2019), and Lugaro cells (Lainé and Axelrad, 1998; Dieudonné and Dumoulin, 2000; Dieudonné, 2001) have been reported. Furthermore, the heterogeneous innervation of 5-HT axons in different layers of the cerebellar cortex (Chan-Palay, 1975) will influence how 5-HT release affects neurons and their interactions within lobule VII. Regardless of the specific cellular targets of 5-HT in lobule VII, our results provide further evidence that this lobule is involved in anxiety by establishing that 5-HT input into this lobule regulates cerebellar-related anxiety behavior bidirectionally. Thus, we conclude that lobule VII is important for anxiety behavior, though this does not preclude contributions from other cerebellar regions.

One surprising conclusion from our experiments is that activating 5-HT input in lobule VII decreases anxiety; this contrasts with previous studies showing that global activation of 5-HT neurons in the dorsal raphe and/or median raphe nuclei increases anxiety (Ohmura et al., 2014; Teissier et al., 2015; Marcinkiewicz et al., 2016; Abela et al., 2020). The different effects of 5-HT in different brain regions leads to the question of the underlying logic for these effects of 5-HT. Perhaps the cerebellar cortex—having an inhibitory output—may exert inhibitory feedback control over the rest of the 5-HT anxiety circuit (Bartolomeo et al., 2022). Such an inhibitory role has already been proposed for other brain areas, such as the ventral hippocampus (Tu et al., 2014). Future experiments will be needed to address this possibility by investigating anxiety pathway components downstream from the cerebellum.

In conclusion, our findings indicate that 5-HT projections into lobule VII connect the cerebellum with the rest of the anxiety circuit, at least for the case of male mice, and that experimental perturbation of this pathway modulates anxiety behavior. Whether 5-HT input in the cerebellum similarly plays a role in regulating anxiety behavior in female mice remains to be

investigated because no equivalent cerebellar anxiety locus has been identified in females: activating MLI activity in lobule VII modulates anxiety output in male mice, but not in female mice (Chin, 2023). Our results also represent the first measurements of endogenous 5-HT signaling in the cerebellum during anxiety behavior. Our work serves as the foundation for future analysis of the role of the cerebellum in regulating anxiety and should stimulate further investigation into the role of neuromodulatory systems in cerebellar function.

References

- Abela AR, Browne CJ, Sargin D, Prevot TD, Ji XD, Li Z, Lambe EK, Fletcher PJ (2020) Median raphe serotonin neurons promote anxiety-like behavior via inputs to the dorsal hippocampus. *Neuropharmacology* 168:107985.
- Andrade TG, Zangrossi H Jr, Graeff FG (2013) The median raphe nucleus in anxiety revisited. *J Psychopharmacol* 27:1107–1115.
- Badura A, Verpeut JL, Metzger JW, Pereira TD, Pisano TJ, Deverett B, Bakshinskaya DE, Wang SS (2018) Normal cognitive and social development require posterior cerebellar activity. *Elife* 7:e36401.
- Baek SJ, Park JS, Kim J, Yamamoto Y, Tanaka-Yamamoto K (2022) VTA-projecting cerebellar neurons mediate stress-dependent depression-like behaviors. *Elife* 11:e72981.
- Bartolomeo P, di Pellegrino G, Chelazzi L (2022) The brain's brake: inhibitory mechanisms in cognition and action. *Cortex* 157:323–326.
- Bishop GA, Ho RH (1985) The distribution and origin of serotonin immunoreactivity in the rat cerebellum. *Brain Res* 331:195–207.
- Bobée S, Mariette E, Tremblay-Leveau H, Caston J (2000) Effects of early midline cerebellar lesion on cognitive and emotional functions in the rat. *Behav Brain Res* 112:107–117.
- Calhoun GG, Tye KM (2015) Resolving the neural circuits of anxiety. *Nat Neurosci* 18:1394–1404.
- Canton-Josh JE, Qin J, Salvo J, Kozorovitskiy Y (2022) Dopaminergic regulation of vestibulo-cerebellar circuits through unipolar brush cells. *Elife* 11:e76912.
- Cardozo Pinto DF, et al. (2019) Characterization of transgenic mouse models targeting neuromodulatory systems reveals organizational principles of the dorsal raphe. *Nat Commun* 10:4633.
- Carta I, Chen CH, Schott AL, Dorizan S, Khodaklah K (2019) Cerebellar modulation of the reward circuitry and social behavior. *Science* 363:eaav0581.
- Cassano GB, Baldini Rossi N, Pini S (2002) Psychopharmacology of anxiety disorders. *Dialogues Clin Neurosci* 4:271–285.
- Cassimjee N, Fouché JP, Burnett M, Lochner C, Warwick J, Dupont P, Stein DJ, Cloete KJ, Carey PD (2010) Changes in regional brain volumes in social anxiety disorder following 12 weeks of treatment with escitalopram. *Metab Brain Dis* 25:369–374.
- Chan-Palay V (1975) Fine structure of labelled axons in the cerebellar cortex and nuclei of rodents and primates after intraventricular infusions with tritiated serotonin. *Anat Embryol* 148:235–265.
- Chao OY, Zhang H, Pathak SS, Huston JP, Yang YM (2021) Functional convergence of motor and social processes in lobule IV/V of the mouse cerebellum. *Cerebellum* 20:836–852.
- Chin PW (2023) Cerebellar modulation of anxiety behavior. Doctoral thesis, Nanyang Technological University, Singapore, Nanyang Technological University, Singapore.
- Chin PW, Augustine GJ (2023) The cerebellum and anxiety. *Front Cell Neurosci* 17:1130505.
- Cutando L, et al. (2022) Cerebellar dopamine D2 receptors regulate social behaviors. *Nat Neurosci* 25:900–911.
- Dean I, Robertson SJ, Edwards FA (2003) Serotonin drives a novel GABAergic synaptic current recorded in rat cerebellar Purkinje cells: a Lugaro cell to Purkinje cell synapse. *J Neurosci* 23:4457–4469.
- Deng F, et al. (2024) Improved green and red GRAB sensors for monitoring spatiotemporal serotonin release in vivo. *Nat Methods* 21:692–702.
- Dieudonné S (2001) Book review: serotonergic neuromodulation in the cerebellar cortex: cellular, synaptic, and molecular basis. *Neuroscientist* 7:207–219.
- Dieudonné S, Dumoulin A (2000) Serotonin-driven long-range inhibitory connections in the cerebellar cortex. *J Neurosci* 20:1837.
- Fernandes CEM, Serafim KR, Gianlorenco ACL, Mattioli R (2017) Intra-vermis H4 receptor agonist impairs performance in anxiety- and fear-mediated models. *Brain Res Bull* 135:179–184.
- Fleming E, Hull C (2019) Serotonin regulates dynamics of cerebellar granule cell activity by modulating tonic inhibition. *J Neurophysiol* 121:105–114.
- Frontera JL, Baba Aissa H, Sala RW, Mailhes-Hamon C, Georgescu IA, Léna C, Popa D (2020) Bidirectional control of fear memories by cerebellar neurons projecting to the ventrolateral periaqueductal grey. *Nat Commun* 11:5207.
- Godlevsky LS, Muratova TN, Kresyun NV, van Luijckelaar G, Coenen AM (2014) Anxiolytic and antidepressive effects of electric stimulation of the paleocerebellar cortex in pentylenetetrazol kindled rats. *Acta Neurobiol Exp* 74:456–464.
- Ha S, et al. (2016) Cerebellar Shank2 regulates excitatory synapse density, motor coordination, and specific repetitive and anxiety-like behaviors. *J Neurosci* 36:12129–12143.
- Helgers SOA, Al Krinawe Y, Alam M, Krauss JK, Schwabe K, Hermann EJ, Al-Afif S (2020) Lesion of the fastigial nucleus in juvenile rats deteriorates rat behavior in adulthood, accompanied by altered neuronal activity in the medial prefrontal cortex. *Neuroscience* 442:29–40.
- Hernandez-Vazquez F, Garduno J, Hernandez-Lopez S (2019) GABAergic modulation of serotonergic neurons in the dorsal raphe nucleus. *Rev Neurosci* 30:289–303.
- Ito M (2002) Historical review of the significance of the cerebellum and the role of Purkinje cells in motor learning. *Ann N Y Acad Sci* 978:273–288.
- Jackman SL, Chen CH, Offermann HL, Drew IR, Harrison BM, Bowman AM, Flick KM, Flaquer I, Regehr WG (2020) Cerebellar Purkinje cell activity modulates aggressive behavior. *Elife* 9:e53229.
- Kim JE, Chae S, Kim S, Jung YJ, Kang MG, Heo W, Kim D (2021) Cerebellar 5HT-2A receptor mediates stress-induced onset of dystonia. *Sci Adv* 7:eabb5735.
- Koeppen AH (2018) The neuropathology of the adult cerebellum. *Handb Clin Neurol* 154:129–149.
- Kuhn B, Ozden I, Lampi Y, Hasan MT, Wang SS (2012) An amplified promoter system for targeted expression of calcium indicator proteins in the cerebellar cortex. *Front Neural Circuits* 6:49.
- Lainé J, Axelrad H (1998) Lugaro cells target basket and stellate cells in the cerebellar cortex. *Neuroreport* 9:2399–2403.
- Li S-J, Wang Y, Strahlendorf HK, Strahlendorf JC (1993) Serotonin alters an inwardly rectifying current (I_h) in rat cerebellar Purkinje cells under voltage clamp. *Brain Res* 617:87–95.
- Longley M, Ballard J, Andres-Alonso M, Varatharajah RC, Cuthbert H, Yeo CH (2021) A patterned architecture of monoaminergic afferents in the cerebellar cortex: noradrenergic and serotonergic fibre distributions within lobules and parasagittal zones. *Neuroscience* 462:106–121.
- Madisen L, et al. (2012) A toolbox of Cre-dependent optogenetic transgenic mice for light-induced activation and silencing. *Nat Neurosci* 15:793–802.
- Marcinkiewicz CA, et al. (2016) Serotonin engages an anxiety and fear-promoting circuit in the extended amygdala. *Nature* 537:97–101.
- Maura G, Roccatagliata E, Ulivi M, Raiteri M (1988) Serotonin-glutamate interaction in rat cerebellum: involvement of 5-HT1 and 5-HT2 receptors. *Eur J Pharmacol* 145:31–38.
- Mendlin A, Martín FJ, Rueter LE, Jacobs BL (1996) Neuronal release of serotonin in the cerebellum of behaving rats: an in vivo microdialysis study. *J Neurochem* 67:617–622.
- Mitoma H, Kobayashi T, Song SY, Konishi S (1994) Enhancement by serotonin of GABA-mediated inhibitory synaptic currents in rat cerebellar Purkinje cells. *Neurosci Lett* 173:127–130.
- Moreno-Rius J (2018) The cerebellum in fear and anxiety-related disorders. *Prog Neuropsychopharmacol Biol Psychiatry* 85:23–32.
- Morton SM, Bastian AJ (2004) Cerebellar control of balance and locomotion. *Neuroscientist* 10:247–259.
- Moulédous L, Roullet P, Guiard BP (2018) Brain circuits regulated by the 5-HT2A receptor: behavioural consequences on anxiety and fear memory. In: *5-HT2A receptors in the central nervous system* (Guiard BP, Di Giovanni G, eds), pp 231–258. Cham: Springer International Publishing.
- Ohmura Y, Tanaka KF, Tsunematsu T, Yamanaka A, Yoshioka M (2014) Optogenetic activation of serotonergic neurons enhances anxiety-like behaviour in mice. *Int J Neuropsychopharmacol* 17:1777–1783.
- Olivier JDA, Olivier B (2020) Translational studies in the complex role of neurotransmitter systems in anxiety and anxiety disorders. In: *Anxiety disorders: rethinking and understanding recent discoveries* (Kim Y-K, ed), pp 121–140. Singapore: Springer Singapore.
- Oostland M, Buijink MR, Teunisse GM, Von Oerthel L, Smidt MP, Van Hooft JA (2014) Distinct temporal expression of 5-HT1A and 5-HT2A receptors on cerebellar granule cells in mice. *Cerebellum* 13:491–500.

- Oostland M, Hooft JAV (2016) Serotonin in the cerebellum. In: *Essentials of cerebellum and cerebellar disorders* (Gruol DL, Koibuchi N, Manto M, Molinari M, Schmammann JD, Shen Y, eds), pp 243–247. Cham, Switzerland: Springer International Publishing.
- Pierce ET, Hoddevik GH, Walberg F (1977) The cerebellar projection from the raphe nuclei in the cat as studied with the method of retrograde transport of horseradish peroxidase. *Anat Embryol* 152:73–87.
- Richter S, Schoch B, Kaiser O, Groetschel H, Dimitrova A, Hein-Kropp C, Maschke M, Gizewski ER, Timmann D (2005) Behavioral and affective changes in children and adolescents with chronic cerebellar lesions. *Neurosci Lett* 381:102–107.
- Roy AK, et al. (2013) Intrinsic functional connectivity of amygdala-based networks in adolescent generalized anxiety disorder. *J Am Acad Child Adolesc Psychiatry* 52:290–299.e2.
- Rudolph S, et al. (2020) Cerebellum-specific deletion of the GABA(A) receptor δ subunit leads to sex-specific disruption of behavior. *Cell Rep* 33:108338.
- Saitow F, Hirono M, Suzuki H (2013) Serotonin and synaptic transmission in the cerebellum. In: *Handbook of the cerebellum and cerebellar disorders* (Manto M, Schmammann JD, Rossi F, Gruol DL, Koibuchi N, eds), pp 915–926. Dordrecht: Springer Netherlands.
- Schindelin J, et al. (2012) Fiji: an open-source platform for biological-image analysis. *Nat Methods* 9:676–682.
- Scott MM, Wylie CJ, Lerch JK, Murphy R, Lobur K, Herlitze S, Jiang W, Conlon RA, Strowbridge BW, Deneris ES (2005) A genetic approach to access serotonin neurons for in vivo and in vitro studies. *Proc Natl Acad Sci U S A* 102:16472–16477.
- Sengupta A, Bocchio M, Bannerman DM, Sharp T, Capogna M (2017) Control of amygdala circuits by 5-HT neurons via 5-HT and glutamate cotransmission. *J Neurosci* 37:1785–1796.
- Shinnar S, Maciewicz RJ, Shofer RJ (1975) A raphe projection to cat cerebellar cortex. *Brain Res* 97:139–143.
- Steinhardt R (2006) Three stages (and a dividend) on my personal road to Ca²⁺ activation at fertilization. *Semin Cell Dev Biol* 17:226–228.
- Supple WF Jr, Leaton RN, Fanselow MS (1987) Effects of cerebellar vermal lesions on species-specific fear responses, neophobia, and taste-aversion learning in rats. *Physiol Behav* 39:579–586.
- Takeuchi Y, Kimura H, Sano Y (1982) Immunohistochemical demonstration of serotonin-containing nerve fibers in the cerebellum. *Cell Tissue Res* 226:1–12.
- Teissier A, Chemiakine A, Inbar B, Bagchi S, Ray RS, Palmiter RD, Dymecki SM, Moore H, Ansorge MS (2015) Activity of raphe serotonergic neurons controls emotional behaviors. *Cell Rep* 13:1965–1976.
- Thach WT, Goodkin HP, Keating JG (1992) The cerebellum and the adaptive coordination of movement. *Annu Rev Neurosci* 15:403–442.
- Tovote P, Fadok JP, Luthi A (2015) Neuronal circuits for fear and anxiety. *Nat Rev Neurosci* 16:317–331.
- Triarhou LC, Ghetti B (1991) Serotonin-immunoreactivity in the cerebellum of two neurological mutant mice and the corresponding wild-type genetic stocks. *J Chem Neuroanat* 4:421–428.
- Tu W, Cook A, Scholl JL, Mears M, Watt MJ, Renner KJ, Forster GL (2014) Serotonin in the ventral hippocampus modulates anxiety-like behavior during amphetamine withdrawal. *Neuroscience* 281:35–43.
- Wang Y, Zhang D, Wang J, Ma J, Lu L, Jin S (2023) Effects of transcranial magnetic stimulation on cerebellar ataxia: a systematic review and meta-analysis. *Front Neurol* 14:1049813.
- Waselus M, Valentino RJ, Van Bockstaele EJ (2011) Collateralized dorsal raphe nucleus projections: a mechanism for the integration of diverse functions during stress. *J Chem Neuroanat* 41:266–280.
- Wong KLL, Nair A, Augustine GJ (2021) Changing the cortical conductor's tempo: neuromodulation of the claustrum. *Front Neural Circuits* 15:658228.
- Zangrossi H, Del Ben CM, Graeff FG, Guimaraes FS (2020) Serotonin panic and anxiety disorders. In: *Handbook of behavioral neuroscience* (Müller CP, Cunningham KA, eds), pp 611–633. Amsterdam, Netherlands: Elsevier.
- Zhu L, Sacco T, Strata P, Sacchetti B (2011) Basolateral amygdala inactivation impairs learning-induced long-term potentiation in the cerebellar cortex. *PLoS One* 6:e16673.